

Auditory cortex projections target the peripheral field representation of primary visual cortex

Amee J. Hall · Stephen G. Lomber

Received: 10 April 2008 / Accepted: 24 June 2008 / Published online: 19 July 2008
© Springer-Verlag 2008

Abstract The purpose of the present study was to identify projections from auditory to visual cortex and their organization. Retrograde tracers were used to identify the sources of auditory cortical projections to primary visual cortex (areas 17 and 18) in adult cats. Two groups of animals were studied. In the first group, large deposits were centered on the lower visual field representation of the vertical meridian located along the area 17 and 18 border. Following tissue processing, characteristic patterns of cell body labeling were identified in extrastriate visual cortex and the visual thalamus (LGN, MIN, & LPI). In auditory cortex, of the four tonotopically-organized regions, neuronal labeling was identified in the supragranular layers of the posterior auditory field (PAF). Little to no labeling was evident in the primary auditory cortex, the anterior auditory field, the ventral posterior auditory field or in the remaining six non-tonotopically organized regions of auditory cortex. In the second group, small deposits were made into the central or peripheral visual field representations of primary visual cortex.

Labeled cells were identified in PAF following deposits into regions of primary visual cortex representing peripheral, but not central, visual field representations. Furthermore, a coarse topography was identified in PAF, with neurons projecting to the upper field representation being located in the gyral portion of PAF and neurons projecting to the lower field representation located in the sulcal portion of PAF. Therefore, direct projections can be identified from tonotopically organized auditory cortex to the earliest stages of visual cortical processing.

Keywords Area 17 · Area 18 · Auditory cortex · Posterior auditory field · WGA-HRP · Multisensory · Cat

Introduction

Sensory systems do not work in isolation. Different sensory inputs must influence each other and be integrated to more completely represent an individual's environment (Bulkin and Groh 2006). However, integration of sensory information has long been proposed to take place only after extensive processing within cortices devoted to a single modality (Jones and Powell 1970; Ghazanfar and Schroeder 2006). After such processing, it is proposed that integration would occur in association cortices outside of sensory-specific cortex (Bavelier and Neville 2002) in areas such as the superior temporal polysensory area (Bruce et al. 1981; Hikosaka et al. 1988; Nosselt et al. 2007) and ventral intraparietal area (Schroeder and Foxe 2002; Schlack et al. 2005; Avillac et al. 2007) of the monkey, and the anterior ectosylvian sulcus (AES; Dehner et al. 2004) in the cat. There is much evidence in support of this view. For example, electrophysiological studies in monkeys have primarily identified multisensory convergence in higher order areas

A. J. Hall
Graduate Program in Neuroscience,
University of Western Ontario, London, ON N6A 5B8, Canada

S. G. Lomber (✉)
Centre for Brain and Mind, Schulich School of Medicine
and Dentistry, Cerebral Systems Laboratory,
Department of Physiology and Pharmacology,
M216 Medical Sciences Building,
University of Western Ontario, London,
ON N6A 5C1, Canada
e-mail: steve.lomber@uwo.ca

S. G. Lomber
Cerebral Systems Laboratory, Department of Psychology,
Faculty of Social Science, University of Western Ontario,
London, ON N6A 5C2, Canada

of parietal, temporal, and frontal cortex (Hyvarinen and Shelepin 1979; Bruce et al. 1981; Rizzolatti et al. 1981; Mazzoni et al. 1996).

However, more recent studies have suggested that multi-sensory integration may occur at early stages of sensory processing in the cerebral cortex (Schroeder et al. 2003; Schroeder and Foxe 2005; Ghazanfar and Schroeder 2006). Studies have provided both anatomical and physiological evidence of visual and somatosensory input into supposed unimodal regions at the secondary and tertiary levels of processing in the auditory hierarchy (Lewis and Van Essen 2000; Schroeder et al. 2001; Schroeder and Foxe 2002; Fu et al. 2003; Cappe and Barone 2005). Furthermore, recent studies have considered the possibility of non-visual cortical projections to primary visual cortex (V1). These studies have focused on the audiovisual cortical projection to V1 and have described direct projections from both core [primary auditory cortex (AI)] and belt areas of auditory cortex (Falchier et al. 2002; Rockland and Ojima 2003; Clavagnier et al. 2004). These projections were described to specifically target the peripheral visual field representations in V1. The presence of direct projections from auditory cortex to the peripheral representation of V1 is of interest because the integration of acoustic and visual signals, at an early level of processing, could serve to enhance perceptual capabilities that could lead to improved detection in the visual periphery.

In the cat, nearly all previous studies have focused on inputs to V1 from other visual cortical structures (eg. Bulter et al. 1984; Symonds and Rosenquist 1984a). Cat V1 consists of both areas 17 and 18 (Tretter et al. 1975). The only studies to consider non-visual cortical projections to V1 have concentrated on exuberant projections that occur during development. Indeed, during development there are robust projections from AI that terminate in V1 (Dehay et al. 1988; Innocenti et al. 1988; Clarke and Innocenti 1990). However, most of these projections are lost by the time the animal reaches adolescence (Dehay et al. 1988; Innocenti et al. 1988; Clarke and Innocenti 1990). Therefore, the purpose of the present study was to ascertain the mature pattern of projections from auditory cortex to V1 (Fig. 1a).

To accomplish this, we examined two groups of cats. In the first group we made large retrograde tracer deposits (spanning both central and peripheral retinotopic representations) in areas 17 and 18. The results from these deposits show that nearly all labeled neurons were contained in the posterior auditory field (PAF). Therefore, in the second group of cats we made small deposits at locations in the central, paracentral, or peripheral visual field to determine if this projection targeted specific representations in V1. Indeed, in this group of animals we found that PAF projections to V1 specifically target neurons that represent sites in

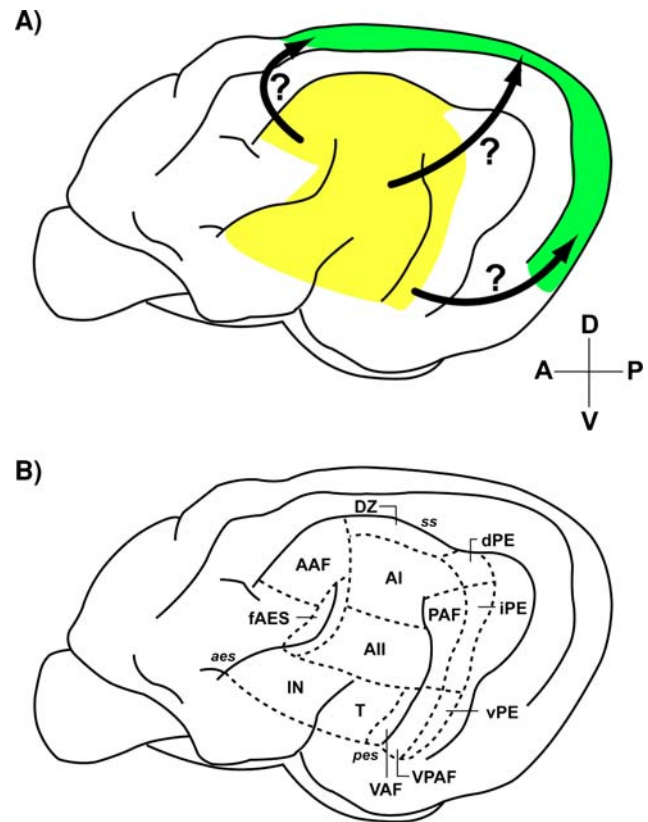


Fig. 1 Lateral views of the left hemisphere of the cat cerebrum. **a** The yellow central region indicates auditory cortex and the green dorsoposterior region highlights primary visual cortex (areas 17 and 18). The purpose of the present study was to identify the origins of auditory projections to primary visual cortex (arrows with question marks). **b** The locations of the ten auditory loci examined. The boundaries of each area are indicated by dashed lines. AI primary auditory field, AII second auditory field, AAF anterior auditory field, fAES auditory field of the anterior ectosylvian sulcus, DZ dorsal zone of auditory cortex, IN insular region, PAF posterior auditory field, T temporal region, VAF ventral auditory field, VPAF ventral posterior auditory field. Sulci are indicated by italics: aes anterior ectosylvian sulcus, pes posterior ectosylvian sulcus, ss suprasylvian sulcus. (A anterior, D dorsal, P posterior, V ventral)

the visual periphery. Finally, we further defined a loose topography in the projections emitting from PAF. Therefore, the present results in the cat are quite similar to those previously identified in the monkey (Falchier et al. 2002; Rockland and Ojima 2003).

Materials and methods

Auditory cortex projections to V1 were examined in 14 mature (>6M) cats (Table 1). Cats were acquired from a commercial laboratory animal breeding facility (Liberty Labs, Waverly, NY). All procedures were conducted in accord with the US National Research Council's *Guidelines for the Care and Use of Mammals in Neuroscience*

Table 1 Retinotopic centers and AP levels of each WGA-HRP deposit into primary visual cortex for each of the 14 cases examined

Case #	Areas targeted	Retinotopic center of deposit (azimuth, elevation)	Tracer deposits (AP levels)	Number of labeled cells in PAF	Number of labeled cells in LPI
B1	Area 17/18	Vertical meridian	P5, P2.5, AP0, A2.5, A5.0, A7.5, A10.0	172	232
B2	Area 17/18	Vertical meridian	P5, P2.5, AP0, A2.5, A5.0, A7.5, A10.0	129	151
C1	Area 17/18	0, -1	P3, P4	3	143
C2	Area 17	2, 2	P4, P5	7	120
PC1	Area 17	5, -1	P3, P2	5	89
PC2	Area 17	10, -5	P1, AP0	12	103
U1	Area 17	0, 20	P7, P8	85	98
U2	Area 17/18	0, 25	P8, P9	72	116
L1	Area 17	5, -35	A13.5, A14.5	69	106
L2	Area 17	5, -35	A13, A14	79	98
L3	Area 17/18	0, -40	A13, A15	116	140
L4	Area 17/18	0, -50	A13, A15	134	151
H1	Area 17	50, -5	P1, A1	135	148
H2	Area 17	30, 10	P3, P5	162	181

Cell counts reflect numbers in every fifth serial section

and Behavioral Research (2003), the Canadian Council on Animal Care's *Guide to the Care and Use of Experimental Animals* (Olfert et al. 1993) and were approved by the University of Western Ontario Animal Use Subcommittee of the University Council on Animal Care.

Two groups of cats were examined. In the first group ($n = 2$), a deposit consisting of seven tracks was made along the dorsal surface of the marginal gyrus which targeted a large area centered on the border between areas 17 and 18 (Payne 1990). These large deposits were directed at the lower vertical meridian of the visual field representation between areas 17 and 18 as described by Tusa et al. (1978, 1979). For the second group ($n = 12$) each cat received smaller deposits, consisting of two tracks, with deposits targeting central ($<2^\circ$, $n = 2$), para-central (2° – 10° , $n = 2$), upper peripheral ($>10^\circ$, $n = 2$), horizontal peripheral ($>10^\circ$, $n = 2$), or lower peripheral ($>10^\circ$, $n = 4$) visual field representations. For most cats (8 of 14), the placement of the tracer deposits was retinotopically defined by electrophysiological recordings made just prior to the tracer deposit (see description below). The retinotopic position of the tracer deposits was not recorded prior to the deposits for the first group of cats that received large tracer deposits along the marginal gyrus (cases B1 and B2), the two para-central deposits (cases PC1 and PC2), and for two of the four lower peripheral deposits (cases L1 and L2; Table 1). For these cases, the retinotopic center of the tracer deposits was determined by comparison with established retinotopic maps of areas 17 and 18 (Tusa et al. 1978, 1979). Furthermore, in these six cases general anesthesia was induced and

maintained using sodium pentobarbital (25 mg/kg iv, or to effect), and not halothane, as described below.

Surgical preparation

Twenty-four hours prior to surgery all cats were fasted, anesthetized with ketamine (20 mg/kg im) to facilitate cannulation of the cephalic vein with an indwelling feline catheter, and an anti-inflammatory medication (dexamethasone, 1.0 mg/kg iv) was administered. On the day of the procedure, general anesthesia was induced with 3% (by volume) halothane in a gaseous mixture of 30% oxygen and 70% nitrous oxide (by volume). A second dose of dexamethasone was given and atropine (0.03 mg/kg sc) was administered to reduce respiratory and alimentary secretions. The epiglottis was sprayed with topical anesthetic (Cetacaine, Cetylite Laboratories, Pennsauken, NJ) and the trachea was intubated with a cuffed endotracheal tube to allow the cat to be ventilated during the electrophysiological recording. The cat's head was supported by a stereotaxic instrument, equipped with a Kopf Model 875 optical investigation unit (David Kopf Instruments, Tujunga, CA), which had a downward tilt of 12.5° . The downward tilt ensured that the visual axis of the eyes were close to horizontal (Bishop et al. 1962).

Heart rate, respiration rate, and rectal temperature were continuously monitored. Body temperature was maintained through the use of a water-filled heating pad. The cat's electrocardiogram was displayed on a monitor. The concentration of halothane inspired by the cat was adjusted to a level

at which the heart rate was stable between 180 and 210 beats/min and a level at which the cat appeared relaxed and showed no signs of arousal, irritation, or increase in heart rate to mildly noxious stimulation such as paw pinching. Under these circumstances, the halothane concentration was invariably between 0.4 and 0.8% of the total inspired gas, and that concentration was taken to be the minimum required for adequate anesthesia during the procedure. The scalp was incised and a craniotomy was made over a region of the marginal gyrus or the posterolateral gyrus.

Eye movements were minimized by intravenous infusion of gallamine triethiodide (Flaxedil, Davison & Gieck, NY). An initial dose of 20 mg/kg was administered via the venous cannula and infused at a rate of 10 mg/kg/h in a 2.5% (by mass) dextrose solution for the duration of the recording experiment. It was found that the initial dose of Flaxedil induces a tachycardia, which persists for the duration of the procedure at a level of 20–40 beats/min above the unparalyzed baseline level. Any increase in heart rate beyond the 20–40 beats/min above the baseline level was immediately counteracted by increasing the concentration of halothane inspired until the heart rate returned to the level indicating an acceptable depth of anesthesia. After paralysis of respiratory muscles by the Flaxedil, the cat was connected to a ventilator and ventilated at rate of 22–28 strokes/min, the expired PCO_2 was monitored with a Surgi-Vet Vital Signs Monitor, and the stroke volume was adjusted to maintain the expired carbon dioxide level at $4.0 \pm 0.2\%$ of the expired gases.

Paralysis of accommodation and pupillary dilation was achieved by topical administration of 1% (w/v) ophthalmic atropine sulfate, and the nictitating membranes were retracted by instilling 1–2 drops of 10% (w/v) phenylephrine hydrochloride into each orbit. The refractive state of each eye was determined by retinoscopy and the appropriate power contact lenses were selected to bring images at a distance of 57 cm from the eye into focus on the retina.

In cases where tracer deposits would be made into the medial wall of area 17, such as para-central, upper peripheral, and horizontal peripheral cases (Table 1), mannitol (1 gm/kg iv) was infused to make cortex more malleable for lateral displacement. With the medial wall of area 17 visible, we were able to use sulcal and gyral landmarks to more accurately place the recording electrode and injection pipette in the desired locations.

Electrophysiological recording

The electrical activity generated by neurons was recorded with insulated tungsten electrodes having exposed tips of 5–10 μm , amplified, filtered through a variable band-pass filter, displayed on an oscilloscope, and monitored aurally.

Mapping was typically done through the eye contralateral to the hemisphere from which activity was recorded. Neurons were activated by projecting rectangular light stimuli of various dimensions onto a perimetric screen. The average illumination for the stimuli was 1.2 logarithmic units above a low photopic background. Outlines of neurons' minimum response fields (Barlow et al. 1967) were plotted and a permanent record of their size, shape, and position made. The positions of neuronal receptive fields were determined with reference to the principle meridians of the visual field. The positions of the meridians were inferred on the screen from the landmarks in the cat's eye projected during the recording session. Important landmarks in the cat's eye, such as the optic disks, vasculature, and area centralis, which appear as dark green regions against the yellow tapetum, were projected repeatedly onto the screen by a fiber optic system (Pettigrew et al. 1979; Payne et al. 1981).

The position of the principle meridians of the visual field were determined by assessment of receptive-field positions, orientation of the eye, and the angular deviation of the area centralis from the center of the blind spot. The position of the vertical midline of the visual field (0° vertical meridian) was calculated from the mean position of several binocular receptive fields of a number of area 17 neurons near the visual axis using the method initially described by Nikara et al. (1968). These mean values were then subtracted from the horizontal distance separating the centers of the two optic disks (Nikara et al. 1968; Joshua and Bishop 1970) and the new value halved to define the position of the 0° vertical meridian for the left and right eye.

Tracer deposits in visual cortex

After the conclusion of the electrophysiological recording procedures to identify the desired retinotopic location of the tracer deposit, anesthesia was deepened, by increasing the concentration of halothane inhaled so as to reduce the heart rate to below 180 beats/min, the infusion of Flaxedil was discontinued, and the cat was prepared for injection of wheat germ agglutinin conjugated to horseradish peroxidase (WGA-HRP).

The electrode was removed from the cortex and replaced with a glass pipette with a 30–35 μm diameter tip. Five percent WGA-HRP was then pressure injected (Nanoliter 2000; World Precision Instruments, Sarasota, FL). For each penetration, two tracer deposits of WGA-HRP (0.1 μl each) were made at ~ 500 and 1,200 μm below the pial surface. All deposits were confined to primary visual cortex (areas 17 and 18; Trepper et al. 1975). The placements, in both anatomical and retinotopic terms, of the different tracer deposits are provided in Table 1.

Following completion of each deposit, the dura was replaced or artificial dura (Gelfilm[®]; Upjohn Co., Kalamazoo,

MI) was placed over the cerebrum. The bone piece was replaced and secured with dental acrylic. Following removal from the stereotaxic apparatus, the cat was ventilated with room air and allowed to recover from the effects of the anesthetic. If necessary, any residual effects of the Flaxedil were antagonized with 0.2 mg neostigmine methylsulphate (Prostigmin, Roche Laboratories, Nutley, NJ) preceded by atropine to obviate spasm (Hammond 1978). An additional administration of dexamethasone and fluids (2.5% dextrose and half-strength lactated ringer solution, 20 ml/kg sc) was provided. The condition of the cat was monitored closely and all cats recovered well, with many eating and drinking within a few hours of revival. Each cat was given (im) a broad spectrum antibiotic (Ultra-pen, Hanford Pharmaceuticals, Syracuse, NY) to counteract any possible infections.

Perfusion and tissue fixation

Forty-eight hours following the tracer deposits each cat was deeply anesthetized with sodium pentobarbital (40 mg/kg, iv). An anti-coagulant [heparin (10,000 U) iv] and a vasodilator [1% sodium nitrite (1 ml iv)] were administered. The cat was then perfused, through the ascending aorta, with 0.1 M phosphate buffered saline (PBS) for 5 min. Next, the arterial system was infused with aldehyde fixatives (1.5% glutaraldehyde/1% paraformaldehyde in 0.1 M PBS) for 20 min. Finally, 10% sucrose in 0.1 M PBS was perfused for 5 min to help cryoprotect the tissue. All solutions were buffered at pH 7.4 and infused at a rate of 100 ml/min. The net effect of the procedures was to exsanguinate the cat, a method which complies with the recommendations of the American Veterinary Medical Association Panel on Euthanasia (Beaver et al. 2001), and to fix tissue for the identification of tracers. The head was then placed in a stereotaxic apparatus, the brain was exposed, blocked at Horsley–Clarke coronal level A22, and removed from the cranium. Each brain was photographed to provide a permanent record and, for cryoprotection, placed in 30% sucrose in 0.1 M PBS until it sunk.

Brains were frozen and coronal sections (50 μ m thick) were cut and collected serially for the entire hemisphere and thalamus. The first series of sections, at 250 μ m intervals, was exposed to tetramethylbenzidine (TMB) and hydrogen peroxide according to the protocol of Olucha et al. (1985) to reveal the presence of WGA-HRP. Series 2 was treated with diaminobenzidine and hydrogen peroxide (Gonatas et al. 1979; Mesulam 1982) to reveal the presence of WGA-HRP. Series 3 was stained with cresyl violet to reveal the presence of Nissl bodies. Series 4 was processed histochemically to demonstrate the presence of cytochrome oxidase using procedures described in previous studies (Payne and Lomber 1996). Selected sections from series 5

were processed for the presence of tracer, as needed, using any of the previously described methods. All histochemically reacted sections were then mounted onto gelatinized glass slides, dehydrated, and coverslipped.

Data collection and analysis

Injection sites were manually plotted on standardized coronal sections adopted from Reinoso-Suárez (1961). The retinotopic extent of the uptake zones was determined by comparison with retinotopic maps of areas 17 and 18 (Tusa et al. 1978, 1979). The laminar extent of each uptake zone was determined by comparison with adjacent sections that were stained for Nissl bodies.

The areas of auditory cortex (Fig. 3) and their lamination were identified using cyto- and myeloarchitectonic features in Nissl (Rose 1949) and myelin (Gallyas 1979) stains, and cytochrome oxidase histochemistry (Payne and Lomber 1996). As done previously (Lomber et al. 1995) the borders in the extrageniculate visual thalamus were identified using myeloarchitectonic methods. We used the nomenclature of Graybiel and Berson (Graybiel 1972; Berson and Graybiel 1978, 1983) to identify the subdivisions of the extrageniculate visual thalamus.

Within the auditory cortex, cell bodies found to contain WGA-HRP were plotted on a standardized flattened rendering adopted from Imig and Reale (1980) and Reale and Imig (1980) containing boundaries for anterior auditory field (AAF), primary auditory field (AI), second auditory field (AII), dorsal zone (DZ), PAF, ventral posterior auditory field (VPAF), and ventral auditory field (VAF). Three other auditory areas of interest; AES (Clarey and Irvine 1986; Meredith and Clemo 1989), IN (Clasca et al. 1997, 2000), and T (Clasca et al. 1997, 2000), were also examined for labeled cells. Laminar distributions of labeled cells were delineated through comparison to surrounding tissue which was stained for Nissl bodies.

Identification and quantification of labeled cells followed several criteria. For a cell to be considered “labeled,” and not an artifact of the reaction process, a nucleus had to be present. Also, the entirety of the soma membrane had to be present. Portions of a cell or remnants of a membrane were not counted. When labeled cells were found on the border of two auditory areas, or in a transitional zone between two areas, the total number of cells in question was evenly distributed to each of the two areas. To more accurately represent the number of labeled cells, numerous focal levels were taken through the z-plane to ensure the full thickness of the section was examined.

For quantitative comparisons, labeled cells in the lateral division of the lateral-posterior (LPI) nucleus were counted on every fifth section in a manner similar to that in auditory cortex. The number of labeled neurons in auditory cortex

were standardized against LPI because it has strong and consistent projections to areas 17 and 18 (Berson and Graybiel 1978; Symonds et al. 1981; Updyke 1983), it contains a well-defined map of the contralateral visual field, including the vertical meridian (Raczkowski and Rosenquest 1981; Hutchins and Updyke 1989), and its borders can be easily distinguished in CO stained sections (Payne and Lomber 1996).

Results

Overview

We examined two groups of animals. In the first group ($n = 2$), a large tracer deposit was made along the dorsal surface of the marginal gyrus that targeted an area centered on the lower vertical meridian visual field representation along the area 17/18 border (Payne 1990). The rationale for such large tracer deposits was to determine if any labeled neurons could be identified in auditory cortex following deposits into V1. The results from these animals are presented in the first part of the results. Once we determined that there were neurons labeled in specific areas of auditory cortex, we next sought to examine if the neurons were targeting specific locations in V1. Therefore, the second group ($n = 12$) of cats received smaller tracer deposits with sub-groups targeting central ($<2^\circ$, $n = 2$), para-central (2° – 10° , $n = 2$), upper peripheral ($>10^\circ$, $n = 2$), horizontal peripheral ($>10^\circ$, $n = 2$), or lower peripheral ($>10^\circ$, $n = 4$) visual field representations. In the final portion of the results we present an analysis of the topography of labeled neurons in auditory cortex as a function of where they project in V1.

Large deposits

Injection sites

In two cases (B1 and B2) seven neighboring penetrations were made along the crown of the marginal gyrus. These deposits resulted in an uptake zone stretching along the dorsal surface of the marginal gyrus (Fig. 2a) from Horsley–Clarke coronal level A11 to P6. In both cases the center of deposit and the uptake zone were confined to primary visual cortex (areas 17 and 18). The deposit sites were similar in both cases. The spread of the deposits extended through all six cortical layers (Fig. 2b). When the uptake zone was compared to previously described retinotopic maps (Tusa et al. 1978, 1979) the deposit site was identified to include a strip of the visual field, along the vertical meridian, extending from an elevation of $\sim +2^\circ$ to $\sim -40^\circ$ (Fig. 2c). Therefore, the large deposits included both central and peripheral visual field representations.

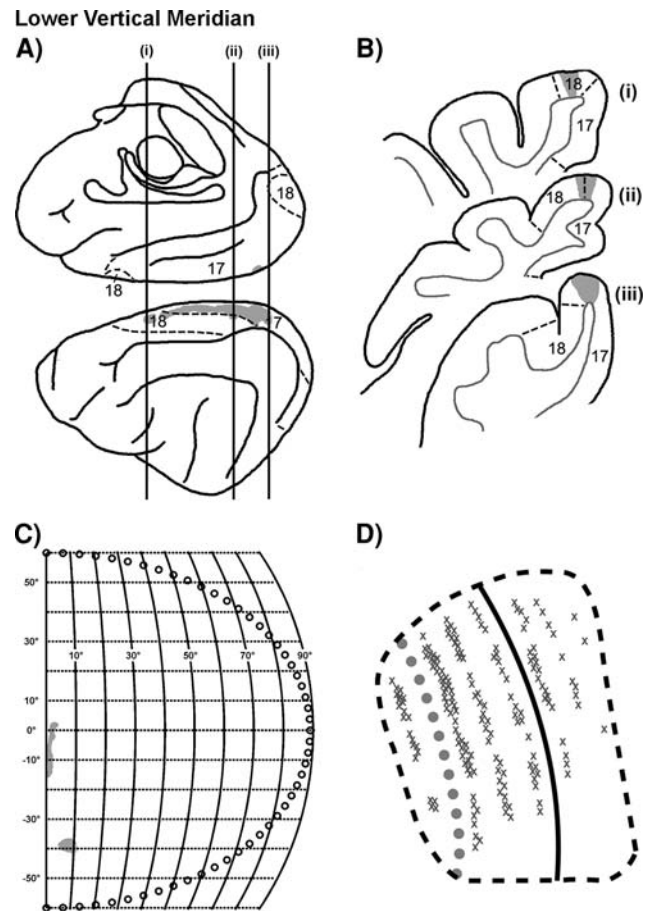


Fig. 2 Large tracer deposits along the area 17/18 border corresponding to the representation of the vertical meridian in the lower visual field. **a** Dorsolateral (*lower*) and medial (*upper*) views of the left hemisphere. *Left* is anterior. Numbered vertical lines show positions of coronal sections in **b**. Dashed lines designate the boundaries of areas 17 and 18. The shaded area specifies the tracer uptake field. **b** Anterior (*i*), middle (*ii*), and posterior (*iii*) coronal sections with tracer uptake field shaded in grey. Thin dark grey lines represent the white-grey matter interface. Solid wide lines indicate the pial surface. *Left* is lateral. **c** Extent of contralateral (*right*) visual field indicated by open circles. The retinotopic location of tracer uptake field (grey shading), as determined by comparison with existing maps (Tusa et al. 1978, 1979). **d** Flattened rendering of PAF. Solid wide black line identifies the posterior lip of the posterior ectosylvian sulcus and the dotted line denotes the fundus. Grey X's indicate individual cells observed within PAF from TMB processed sections. The apparent bands are an artifact of the series sampling interval. *Top* is dorsal and *left* is anterior. Data from case B1

Cell labeling

Ten auditory areas (Fig. 1b) were examined for the presence of labeled cells; AI, AII, AAF, fAES, DZ, IN, PAF, T, VAF, and the VPAF. No area, with the exception of PAF, contained greater than 10% of the total number of labeled cells within auditory cortex (Fig. 3). The largest percentage of labeled cells was found within PAF ($79.1 \pm 5.9\%$; mean \pm SEM). The majority of these cells

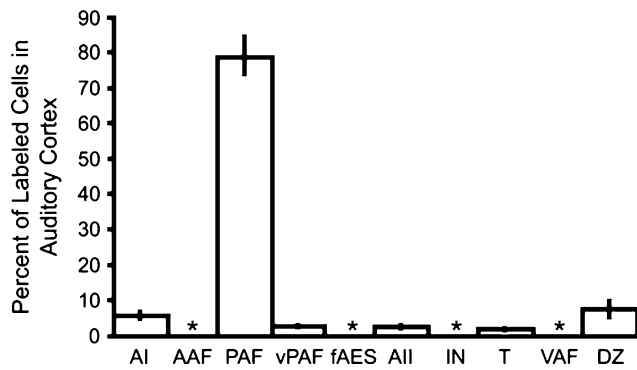


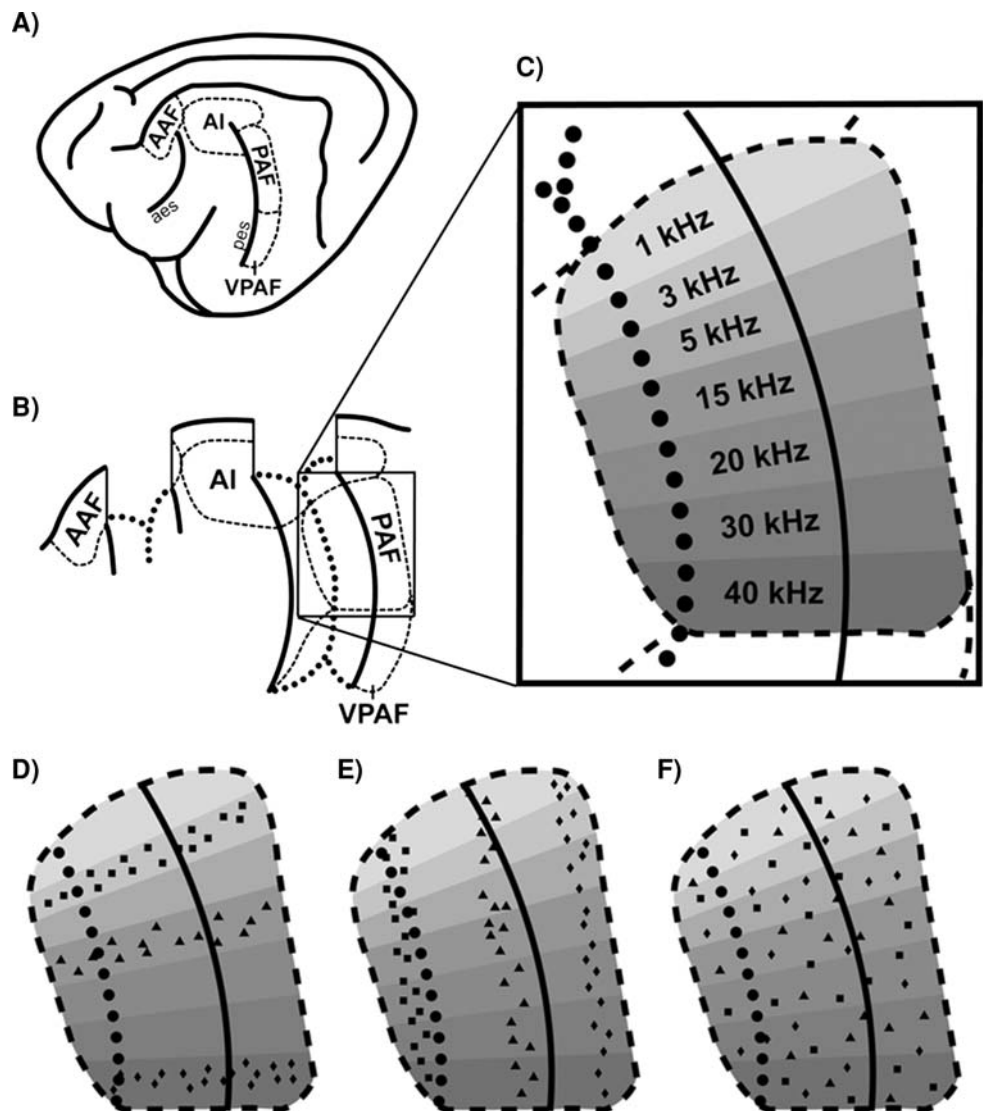
Fig. 3 Histogram showing the percentage of labeled cells in each of the auditory areas, as a function of all labeled neurons in auditory cortex following WGA-HRP deposits along the vertical meridian representation in primary visual cortex. For each area, mean and standard error are provided. Asterisks indicate areas that had less than one percent of labeled cells. Data from cases B1 and B2

(74.6 ± 4.1%) were in the supragranular layers. The area with the second highest percentage of labeled cells was area DZ, which contained 7.6 ± 2.8% of the labeled cells. Many of the auditory areas contained less than 1% of the labeled neurons (AAF, fAES, IN, and VAF; Fig. 3).

With PAF containing the largest number of labeled cells, it became our region of interest. Labeled cells within PAF were plotted onto standardized flattened renderings (Fig. 4c) adopted from Imig and Reale (1980) and Reale and Imig (1980). The result, depicted in Fig. 2d, shows a large number of labeled cells spread throughout PAF with the highest concentration on the posterior bank of the posterior ectosylvian sulcus (the sulcal portion of PAF).

Extrastriate visual areas were also found to have patterns and densities of labeled cells that were characteristic of projections previously identified within extrastriate visual

Fig. 4 Lateral view of the cat cerebrum (a) with the four tonotopic areas outlined. For abbreviations, see Fig. 3. b An expanded, flattened rendering of the four areas. The wide black lines indicate the apertures of the sulci and the dotted lines indicate the sulcal fundi. Grey lines indicate discontinuities on gyral surfaces resulting from flattening. c An enlargement of PAF showing the orientation of frequency bands adapted from Imig and Reale (1980) and Reale and Imig (1980). Three organizational scenarios within PAF were hypothesized following tracer injections into areas 17 and 18. Each symbol corresponds to a hypothetical labeling pattern in PAF following injections at different retinotopic locations in the visual field. d Bands of labeled cells parallel to the frequency bands. e Bands of labeled cells orthogonal to the frequency bands. f Scattered cells throughout PAF



cortex (Symonds and Rosenquist 1984a, b). Characteristic patterns of labeling were also identified within the thalamus (Symonds et al. 1981).

Small deposits

In light of the results from the large deposits, it was apparent that smaller, more specific, deposits were needed to determine any retinotopic specificity to the audiovisual projections. To accomplish this, small deposits were made into specific locations corresponding to central ($<2^\circ$), para-central (2° – 10°), and peripheral ($>10^\circ$) visual field representations in V1.

Central and para-central deposits

Injection sites. The four cases which received small deposits targeted at the central ($n = 2$) or para-central ($n = 2$) visual field representations resulted in small uptake fields confined to the marginal gyrus (Fig. 5Ia, IIa respectively). In both central cases (C1 and C2, Table 1) the injection site was concentrated on the border between areas 17 and 18 at Horsley–Clarke coronal level P3. Both central cases had

similar deposit sites (Fig. 5Ia). The two para-central cases (PC1 and PC2, Table 1) were centered on the marginal gyrus at Horsley–Clarke coronal level AP0, just ventral of the suprasplenic sulcus. These tracer deposits were confined to area 17. Both para-central cases had similar deposit sites (Fig. 5IIa). The spread of both central and para-central deposits extended across all cortical layers (Fig. 5Ib, IIb). When the uptake zone was compared to previously described retinotopic maps (Tusa et al. 1978, 1979) the central deposit was identified to correspond to a small region of the visual field from an elevation of $\sim +2^\circ$ to $\sim -2^\circ$ and extending horizontally $\sim 2^\circ$ (Fig. 5Ic). The para-central deposit was found to be $\sim 2^\circ$ below the horizontal meridian and extended horizontally from $\sim +7^\circ$ to $\sim +14^\circ$ (Fig. 5IIc).

Cell labeling. Cells within PAF were plotted onto the standardized flattened rendering (Fig. 4b, c). The results, depicted in Fig. 5Id, II d show very few labeled cells in PAF (Table 1) in comparison to the large injections. In the other nine areas of auditory cortex relatively low levels of cell labeling, similar to that found in the large deposits, were observed.

In the central and para-central tracer deposit cases, although there were few labeled cells in auditory cortex,

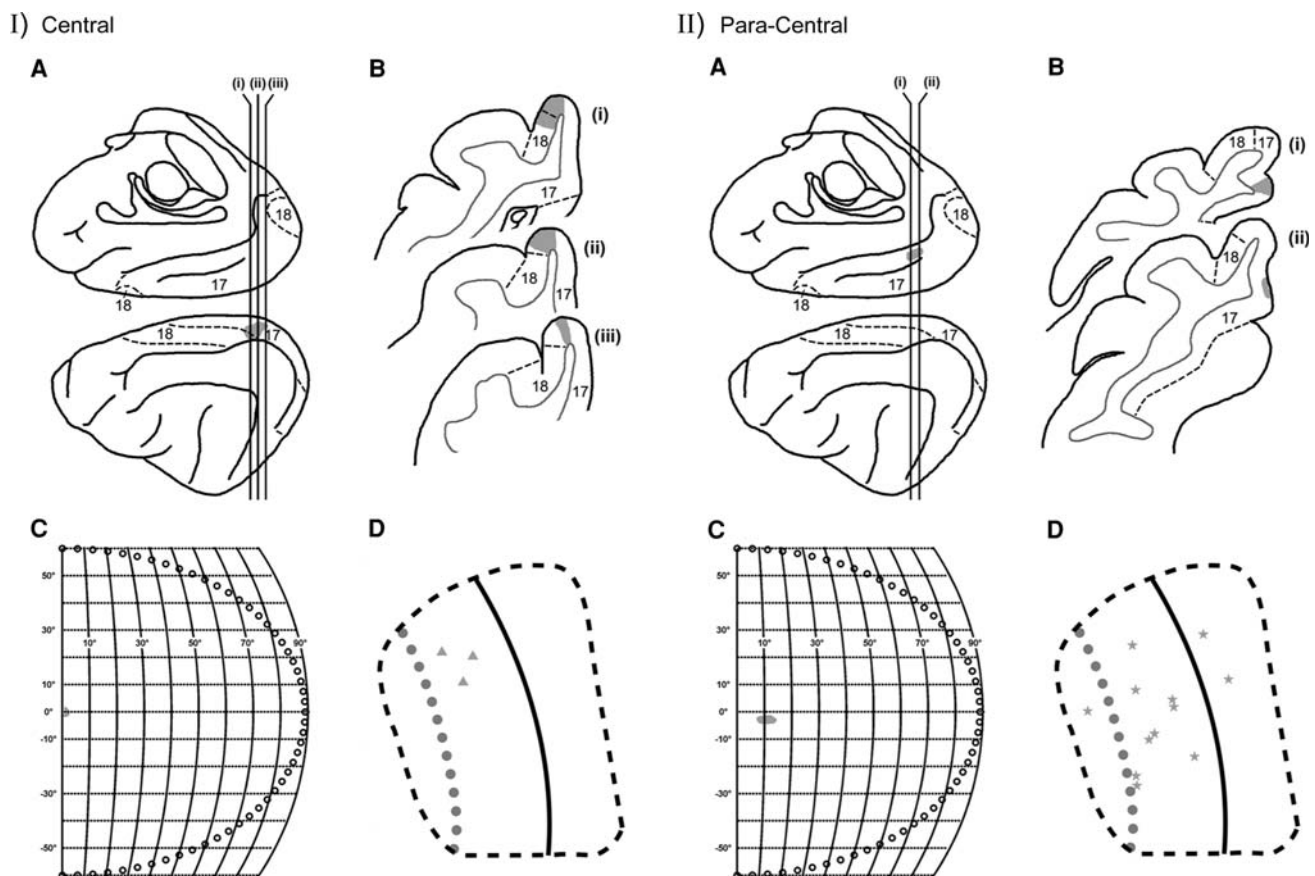


Fig. 5 *I* An example of a tracer deposit in the central ($<2^\circ$) visual field. For conventions see Fig. 2. *d* Grey triangles indicate individual labeled cells identified in PAF. Data from case C1. Note few labeled

neurons. *II* An example of a tracer deposit in the para-central (2° – 10°) visual field. *d* Grey stars indicate individual labeled cells identified in PAF. Data from case PC2. Note few labeled neurons

characteristic densities and patterns of labeling were observed in extrastriate visual areas such as the posteromedial lateral suprasylvian (PMLS; Fig. 6a), posterolateral lateral suprasylvian (PLLS), and anteromedial lateral suprasylvian (AMLS) cortices (Symonds and Rosenquist 1984a, b; Einstein 1996). Characteristic patterns of thalamic labeling were also identified following tracer deposits into the central and para-central representations of V1. Large numbers of labeled cells were observed in layers A, A1, and the C-complex (parvocellular and magnocellular portions of the C-layers) of the dorsal lateral geniculate nucleus (dLGN; Fig. 6b) of the thalamus, the lateral division of the lateral posterior (LPI) nucleus, and the pulvinar nucleus (Symonds et al. 1981). The presence of labeling in thalamic and extrastriate visual cortical areas confirmed the success of the deposits in labeling retrograde pathways. The absence of labeled cells in PAF indicated a weak projection from PAF to the central and para-central visual field representations within V1.

Peripheral deposits

Injection sites. The deposits into the upper peripheral visual field representation (Cases U1 and U2, Table 1) were centered on the ventromedial border of areas 17 and 18 on the marginal gyrus at Horsley–Clarke coronal level P10 (Fig. 7a, b). The spread of the tracer extended throughout all six cortical layers (Fig. 7b) and both cases displayed similar uptake zones. When compared to retinotopic maps of V1 (Tusa et al. 1978, 1979) the deposit site was located on the vertical meridian and extend from an elevation of $\sim +20^\circ$ to $\sim +30^\circ$ (Fig. 7c).

In cases H1 and H2 (Table 1), deposits directed at the horizontal peripheral visual field representation were

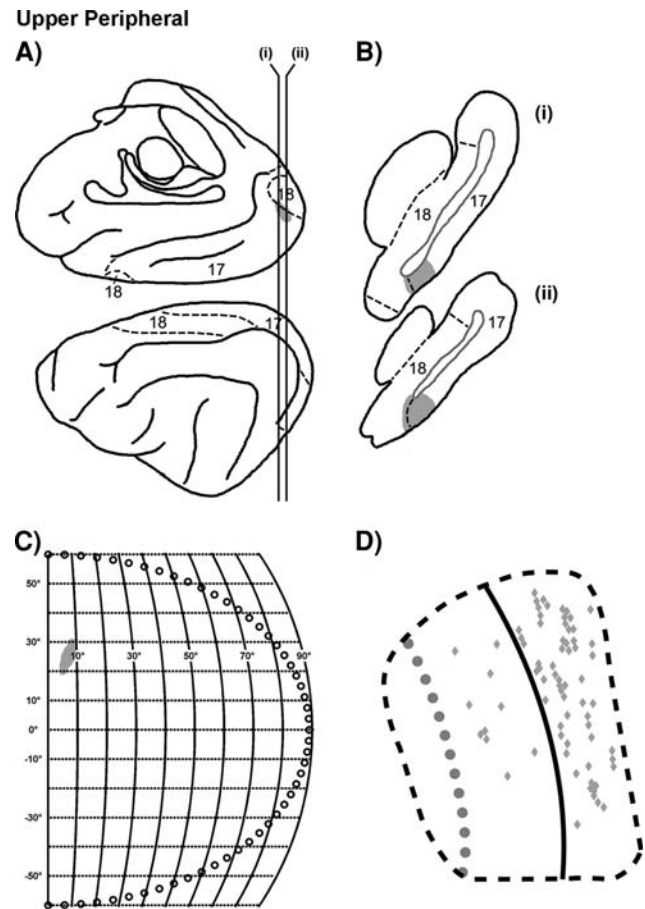


Fig. 7 An example of a tracer deposit in the peripheral ($>10^\circ$) upper visual field. For conventions see Fig. 2. **d** Grey diamonds indicate individual labeled cells identified in PAF. Data from case U2. Note labeled neurons in the gyrus portion of PAF

centered on the dorsal bank of the splenic sulcus at Horsley–Clarke coronal level AP0 (Fig. 8a, b). The spread of the label extended across all cortical layers (Fig. 8b) and

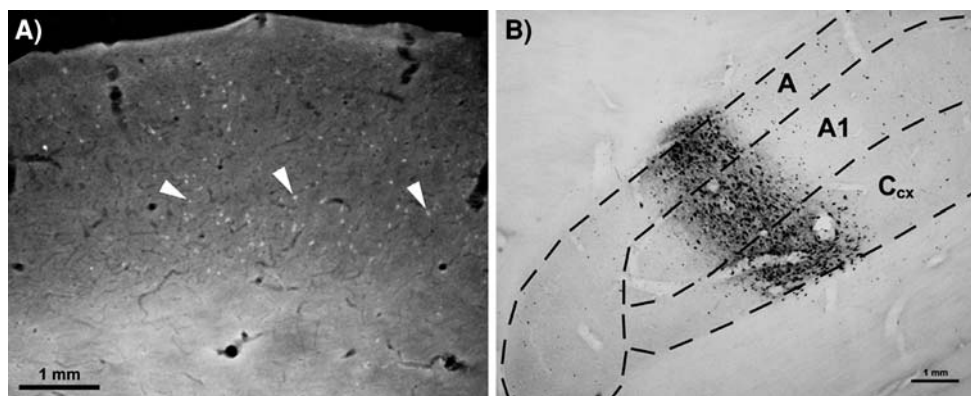


Fig. 6 **a** Darkfield illumination of a coronal section through the posteromedial lateral suprasylvian (PMLS) cortex to show labeled neurons (case PC2). White arrows indicate exemplar labeled cells. Top is pial surface. **b** Coronal section through the left LGN of case PC2 to show large numbers of labeled neurons throughout layers A, A1, and

the C-complex (Ccx) following a paracentral tracer deposit in primary visual cortex. Left is lateral. Although central and para-central deposits labeled few cells in PAF, they did label many neurons in extrastriate visual cortex (**a**) and thalamus (**b**)

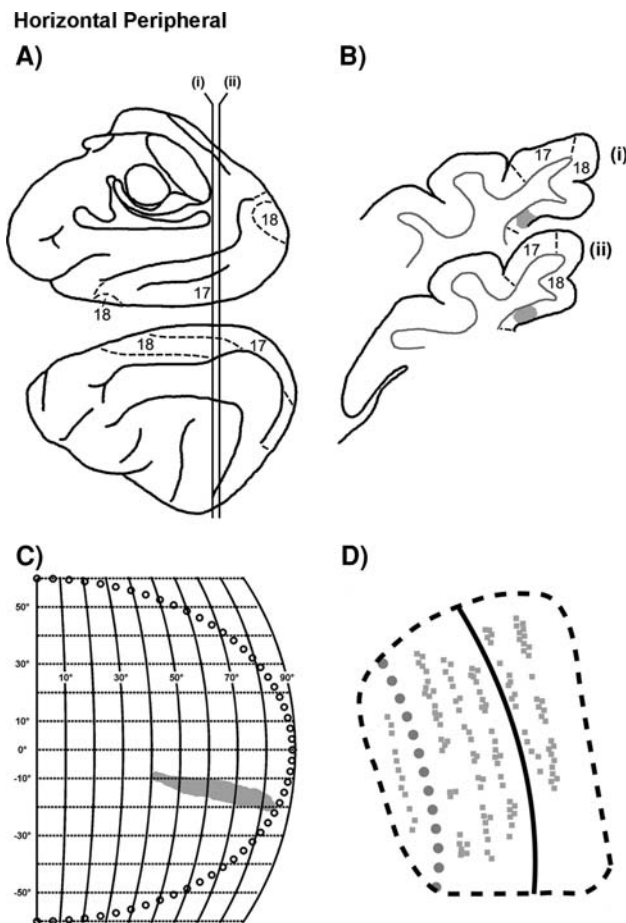


Fig. 8 An example of a tracer deposit in the peripheral ($>10^\circ$) visual field just below the horizontal meridian. For conventions see Fig. 2. **d** Grey squares indicate individual labeled cells identified in PAF. Data from case H1. Note labeled cells throughout PAF

both cases showed similar uptake zones. In retinotopic terms, the deposit site was identified to be at an elevation of $\sim -10^\circ$ and extend horizontally from $\sim 40^\circ$ to $\sim 85^\circ$ (Fig. 8c).

In the four remaining cases (L1–4, Table 1), deposits directed at the lower peripheral field representation were centered on the marginal gyrus at the border between areas 17 and 18 at Horsley–Clarke coronal level A14 (Fig. 9a, b). The spread of the deposits extended throughout all six layers (Fig. 9b) and in all four cases there was little variation in the uptake zones. Retinotopically, the deposit sites extended from an elevation of $\sim -30^\circ$ to $\sim -55^\circ$ (Fig. 9c).

Cell labeling. Overall, similar to the number and distribution of labeled cells in the large deposits, an abundance of labeled cells in PAF were observed following deposits into the upper, horizontal, or lower peripheral field representations of V1. The results of the upper peripheral deposits show a higher number of labeled cells (Table 1) in comparison to the central and para-central deposits (compare Fig. 5d to Fig. 5Id, IIId). The labeled cells are distrib-

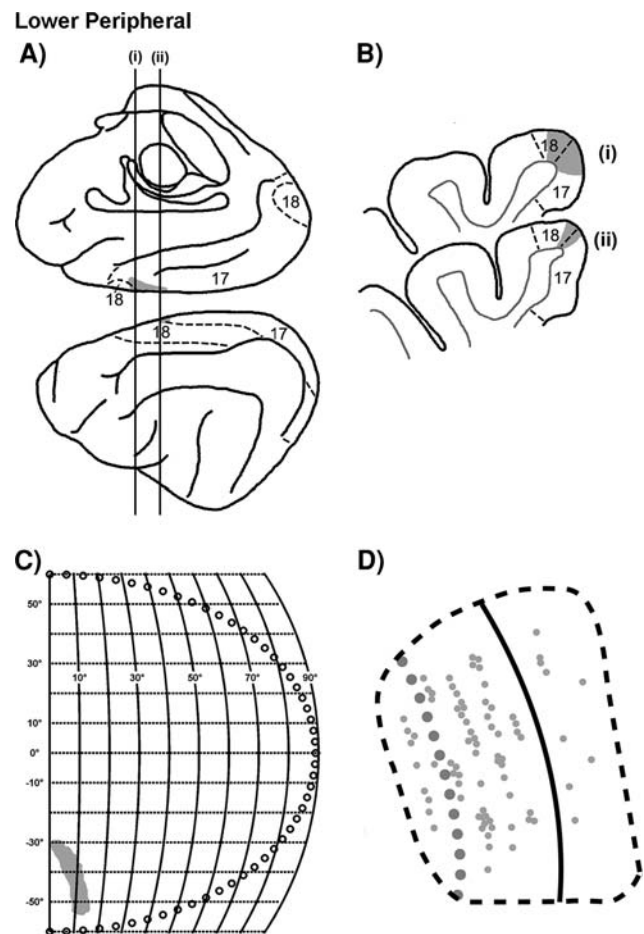


Fig. 9 An example of a tracer deposit in the peripheral ($>10^\circ$) lower visual field. For conventions see Fig. 2. **d** Grey circles indicate individual labeled cells in PAF. Data from case L2. Note labeled cells in the sulcal portion of PAF

uted throughout PAF with a higher concentration located in anterior third of the posterior ectosylvian gyrus (the gyral portion of PAF). In the horizontal peripheral cases the number of labeled cells within PAF, depicted in Fig. 8d, were also much higher (Table 1) than the central and para-central cases. In the horizontal peripheral cases the distribution of labeled cells within PAF appears to be more even (Fig. 8d) than that identified in the upper peripheral cases (Fig. 7d). The third and final group of deposits, made into the lower peripheral visual representation of V1 also resulted in a much higher number of labeled cells (Table 1; Fig. 9d). The labeled cells are distributed throughout PAF with a higher concentration located in the posterior bank of the posterior ectosylvian sulcus (sulcal portion of PAF). Therefore, these results demonstrate that the audiovisual projection from PAF specifically targets the peripheral field representation in V1.

Across all peripheral deposits, the majority of labeled cells were found in the supragranular layers. Therefore, the origin of the projection is not unilaminar. As we did not

examine the termination pattern of this projection in V1, it is impossible to accurately apply a “feedforward” or “feedback” label to this pathway based on the criteria of Fellman and Van Essen (1991).

Similar to the central and para-central tracer deposit cases, characteristic densities and patterns of labeling were observed in extrastriate visual areas following peripheral deposits (Symonds and Rosenquist 1984a, b; Einstein 1996). Similar numbers of labeled cells were also identified in layers A, A1, and the C-complex of the dLGN of the thalamus, and the LPI and pulvinar nuclei (Symonds et al. 1981). For each case, numbers of labeled cells in LPI are provided in Table 1. Therefore, similar labeling patterns were observed in the thalamus regardless of the whether the tracer deposits were centrally or peripherally located.

Comparison of all small deposits. To enable comparison of the percentages of labeled cells between individual cases, the numbers of labeled cells were normalized against a structure that had consistent labeling in all cases. Therefore, the lateral division of the lateral posterior (LPI) nucleus of the thalamus was chosen. The LPI projection to V1 was consistent across all cats and the resulting number

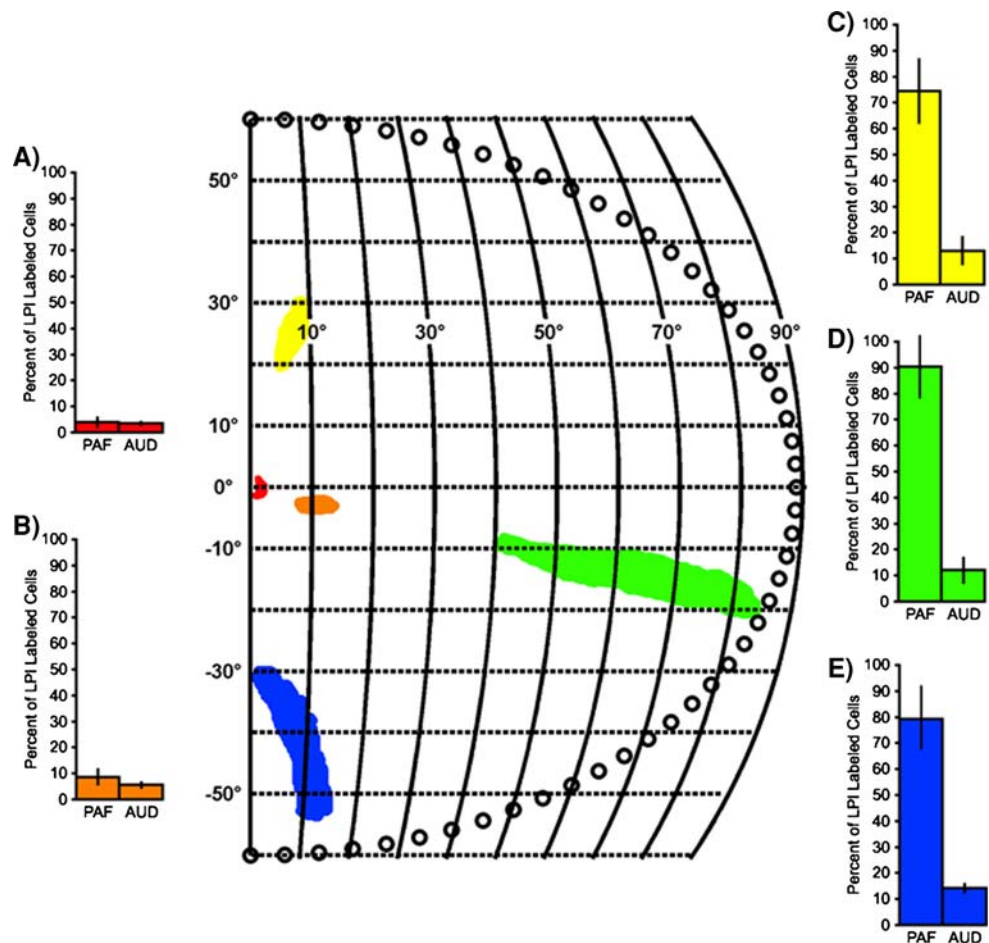
of labeled cells was similar to the larger numbers observed in PAF.

When compared to the number of labeled cells within the LPI, both the central and para-central cases had a small percentage (<10%) of labeled cells within PAF and within the other nine auditory areas examined (AUD; Fig. 10a, b). The three types of peripheral cases (upper, horizontal, and lower), had a large percentage (all >70%) of labeled cells within PAF while the percentage of labeled cells within the other nine auditory areas remained at low levels (Fig. 10c, d, f). These results show that the projection from PAF to V1 specifically targets the peripheral representation of visual space.

PAF to V1 projection organization

PAF is one of four tonotopically organized auditory areas (Fig. 4a; Imig and Reale 1980; Reale and Imig 1980). Within PAF there are bands of cells which respond best to similar frequencies and are organized so that cells responding to lower frequencies are more dorsal while cells responding to higher frequencies are more ventral (Fig. 4c).

Fig. 10 A contralateral (*right*) visual map showing tracer deposits in the central (*red*; <2°), para-central (*orange*; 2°–10°) and peripheral (>10°) upper (*yellow*), horizontal (*green*) and lower (*blue*) visual field representations. Histograms show the percentages of labeled cells as a function of the number of labeled cells in the lateral division of the lateral posterior (LPI) nucleus of the thalamus. Percentage of labeled cells in PAF and all other auditory cortices (AUD) are shown for central (a), para-central (b) and upper peripheral (c), horizontal peripheral (d) and lower peripheral (e) deposits. Histograms show mean percentage and standard errors for all cases. Note the large percentage of labeled cells in PAF following tracer deposits in the peripheral representation of area 17



As V1 has a retinotopic organization (Tusa et al. 1978, 1979), the sites it receives projections from (afferents) and the sites it sends projections to (efferents), also tend to have some form of retinotopic organization (Sanderson 1971; Palmer et al. 1978; Tusa and Palmer 1980; Updyke 1986; Hutchins and Updyke 1989; Grant and Shipp 1991). Therefore, a possible retinotopic organization of the projection to V1, with respect to the tonotopic organization of PAF, was examined. We hypothesized three potential organizational scenarios; (1) bands of labeled cells corresponding to specific retinotopic locations would be found orthogonal to the tonotopic bands in PAF (Fig. 4d). This organization would align specific locations of visual space with given frequencies and thus was considered the least likely. (2) Bands of labeled cells corresponding to specific retinotopic locations would be found perpendicular to the tonotopic bands in PAF (Fig. 4e). (3) Labeled cells corresponding to specific retinotopic locations would be scattered throughout PAF with no apparent organization (Fig. 4f).

The labeled cells in PAF resulting from deposits in the upper, horizontal, and lower peripheral visual field (Fig. 11a) representations are overlaid in Fig. 11b. From this perspective, a loose organization can be observed, with labeled cells projecting to the lower visual field representation (blue) concentrated in the posterior ectosylvian (PE) sulcus, and those cells projecting to the upper visual field representation (yellow) concentrated on the PE gyrus. To quantitatively confirm this observation, labeled cells from each of the peripheral conditions were classified as residing on the PE gyrus or in the PE sulcus and calculated as a percentage of all labeled cells within PAF (Fig. 11c). From this analysis we identified that, within PAF, the majority of cells projecting to the upper peripheral visual field representation in V1 are located on the PE gyrus ($84.3 \pm 1.9\%$), while the majority of cells projecting to the lower peripheral representation are located on the posterior bank of the PE sulcus ($76.9 \pm 4.7\%$). Therefore, the projection from PAF to V1 has a loose topographic organization roughly corresponding to the second hypothesized organizational scenario (Fig. 4e).

Discussion

Summary

In this study we deposited retrograde tracers into V1 and examined auditory cortex to determine the origin of an acoustic projection to V1. Following large deposits along the lower vertical meridian representation of the visual field within V1, a substantially larger number of labeled cells were identified in PAF than the remainder of auditory cortex. Smaller central ($<2^\circ$) and para-central (2° – 10°) depos-

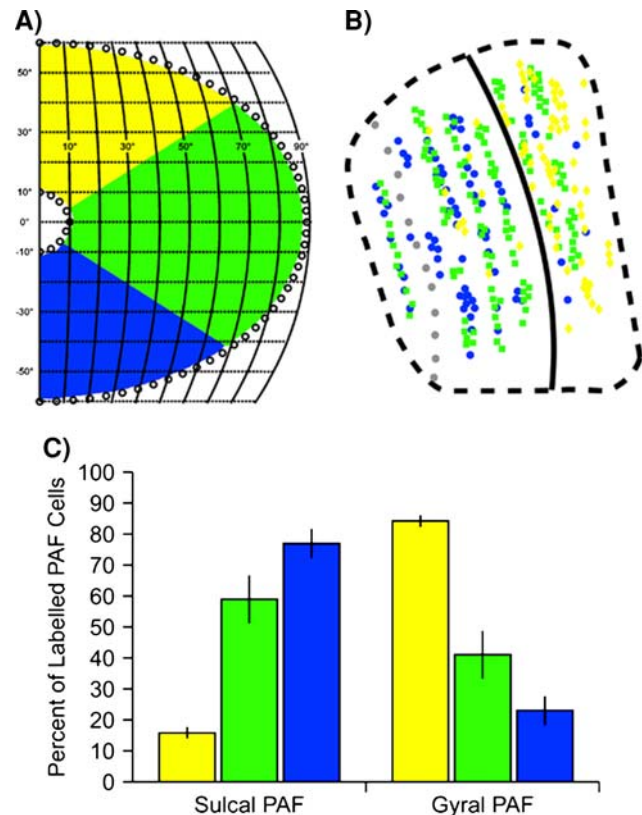


Fig. 11 Organization of labeled cells identified in PAF as a function of the retinotopic location of the tracer deposit. **a** Contralateral (*right*) visual field with peripheral segments dissociated. *Yellow*, *green* and *blue* sections representing upper, horizontal and lower visual fields, respectively. **b** Overlay of the labeled PAF cells identified in three exemplar cases. *Diamonds*, *squares* and *circles* correspond to upper, horizontal and lower peripheral deposits, respectively. **c** Percentage of labeled cells in the sulcal and gyral portions of PAF with relation to the retinotopic position of the tracer deposit. Color coding corresponds to those found in **a**. **c** Histogram shows mean percentage and standard errors for all cases. Cells projecting to the upper peripheral visual field representation tended to be located in the gyral portion of the PAF while cells projecting to the lower peripheral field representation tended to be located in the sulcal portion of PAF

its in V1 resulted in relatively low numbers of labeled cells throughout auditory cortex. However, small peripheral ($>10^\circ$) deposits in V1 resulted in a large number of labeled cells within PAF with small numbers of labeled cells throughout the other auditory areas. Further analysis of the pattern of labeled cells in PAF revealed a loose retinotopic organization in the PAF to V1 projection. Cells projecting to the upper peripheral visual field representation are concentrated on the gyral portion of PAF and cells projecting to the lower peripheral visual field representation are concentrated in the sulcal portion of PAF. Therefore, the projection from PAF to the peripheral visual field representation of V1 is robust and is organized in a coarse spatial map within PAF.

Heteromodal connections

In examining cortical connections, most studies focus on projections within a particular modality. Indeed, such is the case in the cat, with nearly all previous studies focusing on inputs to primary visual cortex from other visual cortical structures (eg. Bullier et al. 1984; Symonds and Rosenquist 1984a). The only studies to examine non-visual cortical projections to V1 have concentrated on the development of these projections. Overall, these studies have reported dense exuberant projections from auditory cortex to V1 during postnatal development (Clarke and Innocenti 1986; Dehay et al. 1988; Innocenti and Clarke 1984). However, over time, these projections are lost and only a meager number remain by the time the animal reaches adolescence (Clarke and Innocenti 1986; Innocenti et al. 1988). The results from these investigations beg the question as to why the PAF to V1 projection was not readily identified in these earlier studies. It is likely that the answer to this question lies in the specificity of the projection. The present study identified audiovisual projections to the peripheral representation in V1. The exposed and most accessible portion of V1 is the central visual field representation lying along the crown of the marginal gyrus (Tusa et al. 1978, 1979). Therefore, it is likely that the retrograde tracer deposits made in these earlier studies were not large enough to include the peripheral field representations in V1, thus not labeling this projection.

Studies of projections from auditory cortex to V1, in the mature cat, confirm the present observations. Deposits of anterograde tracers into areas AI and AII of cats older than 34 postnatal days results in few, if any, labeled axons in V1 (Innocenti et al. 1988). This finding supports the results of the present study which found that, regardless of the retinotopic position of the retrograde tracer deposit in V1, few neurons were labeled in areas AI or AII. Therefore, previous studies of the audiovisual projection in cats support the present findings.

The present study helps our understanding of the mechanisms underlying multisensory integration as the results confirm the probable generalization across species (carnivores, non-human primates, humans) of a direct link between the auditory cortex and the peripheral visual representation in V1. The present findings closely match similar observations concerning audiovisual projections in the monkey. In these studies, projections from auditory association cortex within the caudal parabelt (CPB) were identified terminating in the peripheral visual field representation of V1 (Fig. 12a; Clavagnier et al. 2004; Falchier et al. 2002; Rockland and Ojima 2003). Furthermore, in the monkey, meager auditory cortex projections to the central visual field representation of V1 were identified. Therefore, in both cats and monkeys, projections from posterior regions

of auditory cortex target the peripheral field representation in V1 (Fig. 12).

In the visual system, the density and pattern of the connections between individual visual areas differ when they involve the central or peripheral visual field representation (Shipp and Zeki 1989; Kaas and Morel 1993; Schall et al. 1995; Galletti et al. 2001; Falchier et al. 2002; Palmer and Rosa 2006). Similarly, the present study and the work of others demonstrate that auditory and multimodal projections to area V1 are restricted to the peripheral visual field representation of the visual field (present study; Falchier et al. 2002). Furthermore, in the somatosensory system there is evidence of a different connectivity pattern that corresponds to the body representation, especially in terms of the density of connections between areas (Krubitzer and Kaas 1990; Huffman and Krubitzer 2001). Cappe and Barone (2005) demonstrated that heteromodal connections might also be specific to the sensory representation. They found that projections from ventral and dorsal fundus of the superior temporal area of the monkey are selective for the body part representation in areas 1/3b (Cappe and Barone 2005). Taken together, these results suggest that a primary sensory area is heterogeneous in terms of areal connectivity, suggesting a regional functional specialization. Finally, these results also confirm that the connectivity of a single cortical region depends on its sensory representation.

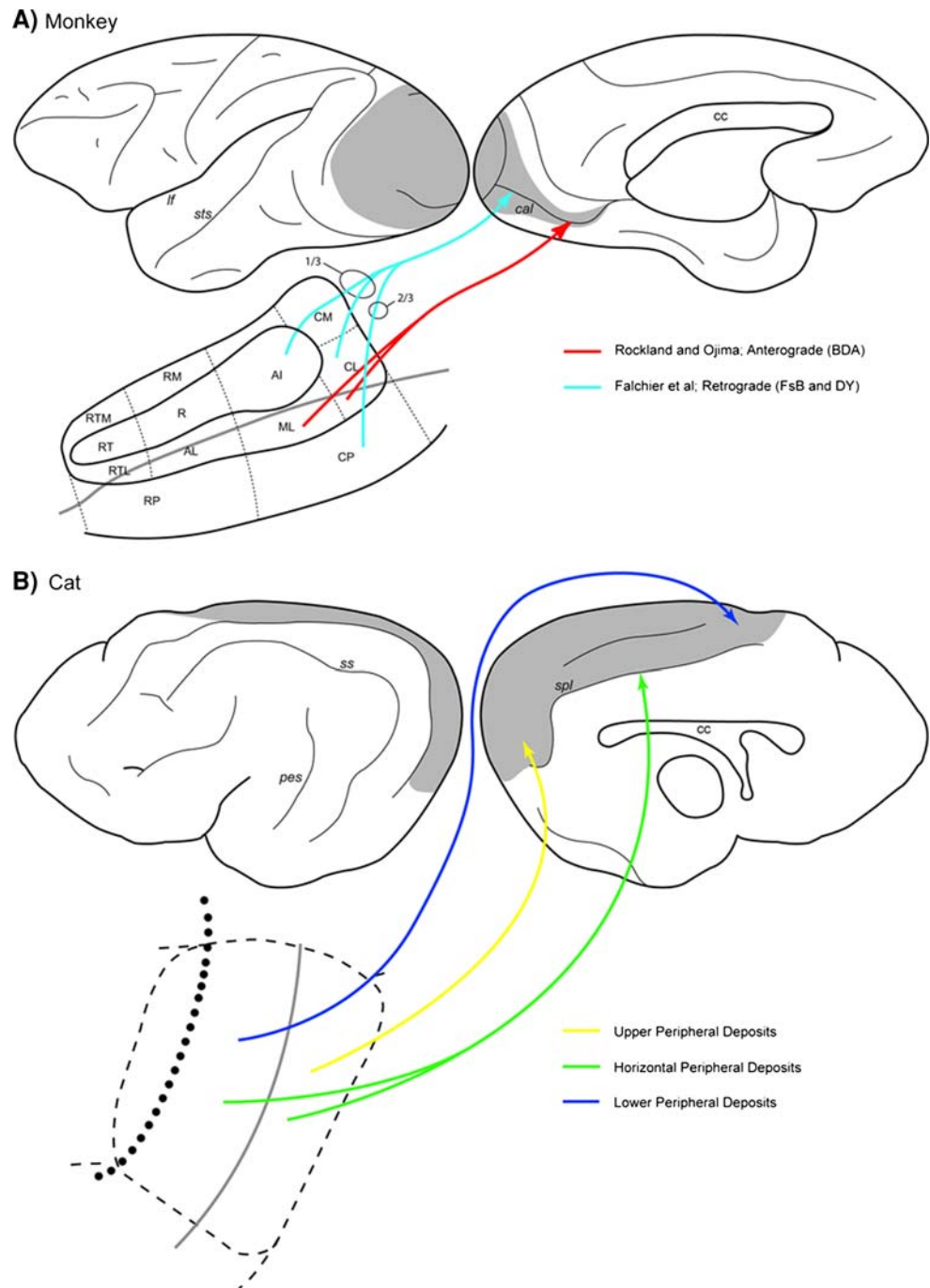
Is the projection reciprocal?

Within visual or auditory cortex, projections between areas are largely reciprocal (Rockland and Pandya 1979; Lee and Winer 2008) with only a small number being identified as unidirectional (Felleman and Van Essen 1991). Thus, it is conceivable that reciprocal projections, arising in V1 and projecting to posterior auditory cortex, may exist. However, earlier studies in the cat failed to identify a direct projection from V1 to PAF (Innocenti and Clarke 1984; Innocenti et al. 1988). Furthermore, Falchier et al. (2002) specifically tested for the possibility of reciprocal connections by placing retrograde tracers into auditory cortex of the monkey and failed to label any neurons in area 17. Although in the present study we did not specifically examine the possibility of reciprocal projections to auditory cortex from V1, their existence appears unlikely. While there are projections from higher-order visual areas to auditory cortex (Rockland and Ojima 2003), there is no evidence of any projections from V1 to auditory cortex. Thus, the pathway from PAF to V1 appears to be unidirectional.

Significance of the pathway origin

In humans, monkeys, and cats, the posterior region of auditory cortex has been shown to be important for the accurate

Fig. 12 Audiovisual pathways terminating in primary visual cortex of the monkey (a) and cat (b). Grey areas on the medial (right) and lateral (left) views indicate primary visual cortex (V1). Dashed lines indicated auditory area boundaries, dotted lines indicate the sulcal fundus, and thin grey lines indicate the lip of the sulcus. Falchier et al. (2002) reported that one-third (1/3) of the projection from auditory cortex originated from the core (AI) and caudolateral (CL) belt and two-thirds (2/3) originated from the caudal parabelt (CP). AI primary auditory cortex, AL anterior lateral auditory belt, CC corpus callosum, CL caudal lateral auditory belt, CM caudomedial auditory belt, CP caudal auditory parabelt, ML middle lateral auditory belt, R rostral area, RM rostromedial auditory belt, RP rostral auditory parabelt, RT rostromedial auditory belt, RTM medial rostromedial auditory belt. Sulci are indicated by italics: *aes* anterior ectosylvian sulcus, *cal* calcarine sulcus, *lf* lateral fissure, *pes* posterior ectosylvian sulcus, *spl* splenial sulcus, *sts* superior temporal sulcus



localization of a sound source. In human subjects, studies of sound localization have identified posterior auditory cortex activation during functional imaging (Ahveninen et al. 2006; Griffiths et al. 1998; Krumbholz et al. 2005), and spatial deficits have been identified in patients with damage to posterior auditory cortex (Clarke et al. 2000). Recently, in a 38 study meta-analysis, Arnott et al. (2004) reviewed evidence from fMRI and PET studies and identified that the majority of the studies found “posterior” activation when subjects performed acoustic spatial tasks. In the monkey, electrophysiological studies have identified neurons in

posterior auditory cortex to be selective for sound localization perception (Rauschecker 1998a, b; Tian et al. 2001). Moreover, the CPB has strong connections with the caudomedial (CM) and caudolateral (CL) areas of the auditory belt (Hackett et al. 1998; Kaas and Hackett 1998, 2000), both of which are employed during auditory localization (Recanzone 2000; Tian et al. 2001). The presence of these dense interconnections has led others to propose that the CPB is especially suited for spatial processing of auditory information (Clavagnier et al. 2004; Kaas and Hackett 2000). Finally, in the cat, both electrophysiological and

behavioral studies have demonstrated the importance of posterior auditory cortex, specifically PAF, to sound localization function (Malhotra et al. 2004; Malhotra and Lomber 2007; Stecker et al. 2003). Therefore, in humans, monkeys, and cats, regions of posterior auditory cortex play a significant role in sound localization.

Of all the areas in auditory cortex that could give rise to a projection to V1, it is intriguing that the projection originates from PAF. Reversible deactivation of PAF produces profound sound localization deficits (Malhotra et al. 2004; Malhotra and Lomber 2007) and of all the auditory areas that contribute to sound localization, it appears to make the largest contribution (Malhotra et al. 2008). Likewise, removal of V1 in the cat produces severe visual localization deficits (Shupert et al. 1993). Overall, the audiovisual pathway described in this study provides a direct link between the region of auditory cortex most responsible for acoustic localization, and a region of visual cortex responsible for accurate visual localization. We propose that this pathway may be involved in either the enhancement or reduction of visual localization functions in the peripheral visual field in the presence of a novel acoustic stimulus.

Significance of the PAF to V1 pathway

The integration of sensory information has long been proposed to occur only after processing within cortices devoted to a single modality. After such processing, it is proposed that multisensory integration occurs in association cortices outside of sensory specific cortex (Bavelier and Neville 2002). However, more recent studies have suggested that multisensory integration may occur at early stages of visual processing in the cerebrum (Ghazanfar and Schroeder 2006; Schroeder et al. 2003; Schroeder and Foxe 2005). For example, studies in human subjects have reported V1 activity in response to acoustic stimulation (Giard and Peronnet 1999; Noesselt et al. 2007). In fact, Watkins et al. (2007) noted that not only was activity higher in V1 when an acoustic stimulus was present but that the area of heightened activity was located in the region of V1 corresponding to the perceived location of a stimulus. However, the origin of this input has remained elusive. In light of this, we would propose that when active, this pathway could show retinotopically specific activity in V1 similar to that observed by Watkins et al. (2007) and may make significant contributions to multisensory integration at the earliest levels of visual cortical processing.

Heteromodal projections to V1 in the blind

The existence of heteromodal connections at early stages in sensory processing has important implications for understanding functional reorganization following sensory

deprivation such as blindness. The human neuro-imaging literature has numerous examples of blind subjects that display activation of V1 while performing somatosensory or acoustic tasks (Buchel et al. 1998; Roder et al. 2002; Weeks et al. 2004; Burton et al. 2002, 2004; Raz et al. 2005; Burton and McLaren 2006; Noppeney 2007). It has been proposed that projections from somatosensory and auditory cortex are “dormant” in sighted subjects and become activated during training on somatosensory or acoustic tasks (Ptito and Kupers 2005; Ptito et al. 2008). Thus, the pathway described in the present study may become more functionally significant during conditions of visual impairment. It may also be that this pathway is amplified in subjects that are congenitally blind or lose sight during early development as a consequence of a peripheral sensory loss.

Acknowledgments We would like to thank Jeffrey Mellott for assistance with the preparation of the tissue. This research was supported by grants from the Canadian Institutes of Health Research and the Natural Science and Engineering Research Council of Canada.

References

- Ahveninen J, Jaaskelainen IP, Rajj T, Bonmassar G, Devore S, Hamalainen M, Levanen S, Lin FH, Sams M, Sinn-Cunningham BG, Witzel T, Belliveau JW (2006) Task-modulated “what” and “where” pathways in human auditory cortex. *Proc Natl Acad Sci USA* 103:14608–14613
- Arnott SR, Binns MA, Grady CL, Alain C (2004) Assessing the auditory dual-pathway model in humans. *Neuroimage* 22:401–408
- Avillac M, Hamed SB, Duhamel J-R (2007) Multisensory integration in the ventral intraparietal area of the macaque monkey. *J Neurosci* 27:1922–1932
- Barlow HB, Blakemore C, Pettigrew JD (1967) The neural mechanisms of binocular depth discrimination. *J Physiol* 193:327–342
- Bavelier D, Neville HJ (2002) Cross-modal plasticity: where and how? *Nat Rev Neurosci* 3:443–452
- Beaver BV, Reed W, Leary S, McKiernan B, Bain F, Schultz R, Bennett BT, Pascoe P, Shull E, Cork LC, Francis-Floyd R, Amass KD, Johnson RJ, Schmidt RG, Underwood W, Thornton GW, Kohn B (2001) 2000 Report of the American Veterinary Medical Association Panel on Euthanasia. *J Am Vet Med Assoc* 218:669–696
- Berson DM, Graybiel AM (1978) Parallel thalamic zones in the LP-pulvinar complex of the cat identified by their afferent and efferent connection. *Brain Res* 147:139–148
- Berson DM, Graybiel AM (1983) Organization of the striate-recipient zone of the cats lateralis posterior-pulvinar complex and its relations with the geniculostriate system. *Neuroscience* 9:337–372
- Bishop PO, Kozak W, Vakkur GJ (1962) Some quantitative aspects of the cat’s eye: axis and plane of reference, visual field coordinates, and optics. *J Physiol* 163:466–502
- Bruce C, Desimone R, Gross CG (1981) Visual properties of neurons in a polysensory area in superior temporal sulcus of the macaque. *J Neurophysiol* 46:369–384
- Buchel C, Price C, Friston K (1998) A multimodal language region in the ventral visual pathway. *Nature* 394:274–277
- Bulkin DA, Groh JM (2006) Seeing sounds: visual and auditory interactions in the brain. *Curr Opin Neurobiol* 16:415–419

- Bullier J, Kennedy G, Salinger W (1984) Branching and laminar origin of projections between visual cortical areas in the cat. *J Comp Neurol* 228:329–341
- Burton H, McLaren DG (2006) Visual cortex activation in late-onset Braille naïve blind individuals: an fMRI study during semantic and phonological tasks with heard words. *Neurosci Lett* 392:38–42
- Burton G, Snyder AZ, Conturo TE, Akbudak E, Ollinger JM, Raichle ME (2002) Adaptive changes in early and late blind: a fMRI study of Braille reading. *J Neurophys* 87:589–607
- Burton G, Sinclair RJ, McLaren DG (2004) Cortical activity to vibrotactile stimulation: an fMRI study in blind and sighted individuals. *Hum Brain Mapp* 23:210–228
- Cappe C, Barone P (2005) Heteromodal connections supporting multisensory integration at low levels of cortical processing in the monkey. *Eur J NeuroSci* 22:2886–2902
- Clarey JC, Irvine DRF (1986) Auditory response properties of neurons in the anterior ectosylvian sulcus of the cat. *Brain Res* 386:12–19
- Clarke S, Innocenti GM (1986) Organization of immature intrahemispheric connections. *J Comp Neurol* 251:1–22
- Clarke S, Innocenti GM (1990) Auditory neurons with transitory axons to visual areas form short permanent projections. *Eur J NeuroSci* 2:227–242
- Clarke S, Bellmann A, Meuli RA, Assal G, Steck AJ (2000) Auditory agnosia and auditory spatial deficits following left hemispheric lesions: evidence for distinct processing. *Neuropsychologia* 28:797–807
- Clasca F, Llamas A, Reinoso-Suárez F (1997) Insular cortex and neighboring fields in the cat: a redefinition based on cortical microarchitecture and connections with the thalamus. *J Comp Neurol* 384:456–482
- Clasca F, Llamas A, Reinoso-Suárez F (2000) Cortical connections of the insular and adjacent parieto-temporal fields in the cat. *Cereb Cortex* 10:371–399
- Clavagnier S, Falchier A, Kennedy H (2004) Long-distance feedback projections to area V1: implications for multisensory integration, spatial awareness, and visual consciousness. *Cogn Affect Behav Neurosci* 4:117–126
- Dehay C, Kennedy H, Bullier J (1988) Characterization of transient cortical projections from auditory, somatosensory, and motor cortices to visual areas 17, 18, and 19 in the kitten. *J Comp Neurol* 272:68–89
- Dehner LR, Keniston LP, Clemo HR, Meredith MA (2004) Cross-modal circuitry between auditory and somatosensory areas of the cat anterior ectosylvian sulcal cortex: a ‘new’ inhibitory form of multisensory convergence. *Cereb Cortex* 14:387–403
- Einstein G (1996) Reciprocal projections of cat extrastriate cortex: I. Distribution and morphology of neurons projecting from posterior medial lateral suprasylvian sulcus to area 17. *J Comp Neurol* 376:518–529
- Falchier A, Clavagnier S, Barone P, Kennedy G (2002) Anatomical evidence of multimodal integration in primate striate cortex. *J Neurosci* 22:5749–5759
- Felleman DJ, Van Essen DC (1991) Distributed hierarchical processing in the primate cerebral cortex. *Cereb Cortex* 1:1–47
- Fu K-MG, Johnston TA, Shah AS, Arnold L, Smiley J, Hackett TA, Garraghty PE, Schroeder CE (2003) Auditory cortical neurons respond to somatosensory stimulation. *J Neurosci* 23:7510–7515
- Galletti C, Gamberini M, Kutz DF, Fattori P, Luppino G, Matelli M (2001) The cortical connections of area V6: an occipito-parietal network processing visual information. *Eur J NeuroSci* 13:1572–1588
- Gallyas F (1979) Silver staining of myelin by means of physical development. *Neurol Res* 1:203–209
- Ghazanfar AA, Schroeder CE (2006) Is neocortex essentially multisensory? *Trends Cogn Sci* 10:278–285
- Giard MH, Peronnet F (1999) Auditory–visual integration during multimodal object recognition in humans: a behavioral and electrophysiological study. *J Cogn Neurosci* 11:473–490
- Gonatas NK, Harper C, Mizutani T, Gonatas JO (1979) Superior sensitivity of conjugates of horseradish peroxidase with wheat germ agglutinin for studies of retrograde axonal transport. *J Histochem Cytochem* 27:728–734
- Grant S, Shipp S (1991) Visuoatopic organization of the lateral suprasylvian area and of an adjacent area of the ectosylvian gyrus of the cat cortex: a physiological and connective study. *Vis Neurosci* 6:315–338
- Graybiel AM (1972) Some extrageniculate visual pathways in the cat. *Invest Ophthalmol* 11:322–332
- Griffiths TD, Buchel C, Frackowiak RS, Patterson RD (1998) Analysis of temporal structure in sound by the human brain. *Nat Neurosci* 1:422–427
- Hackett TA, Stepniewska I, Kaas JH (1998) Subdivisions of auditory cortex and ipsilateral cortical connections of the parabelt auditory cortex in macaque monkeys. *J Comp Neurol* 394:475–495
- Hammond P (1978) Inadequacy of nitrous oxide/oxygen mixtures for maintaining anaesthesia in cats: satisfactory alternatives. *Pain* 5:143–151
- Hikosaka K, Iwai E, Saito HA, Tanaka K (1988) Polysensory properties of neurons in the anterior bank of the caudal superior temporal sulcus of the macaque monkey. *J Neurophys* 60:1615–1637
- Huffman KJ, Krubitzer L (2001) Area 3a: topographic organization and cortical connections in marmoset monkeys. *Cereb Cortex* 11:849–867
- Hutchins B, Updyke BV (1989) Retinotopic organization within the lateral posterior complex of the cat. *J Comp Neurol* 285:350–398
- Hyvarinen J, Shelepin Y (1979) Distribution of visual and somatic functions in the parietal associative area 7 of the monkey. *Brain Res* 169:561–564
- Imig TJ, Reale RA (1980) Patterns of cortico-cortical connections related to Tonotopic maps in cat auditory cortex. *J Comp Neurol* 192:293–332
- Innocenti GM, Clarke S (1984) Bilateral transitory projection to visual areas from auditory cortex in kittens. *Brain Res Dev Brain Res* 14:143–148
- Innocenti GM, Berbel P, Clarke S (1988) Development of projections from auditory to visual areas in the cat. *J Comp Neurol* 272:242–259
- Jones EG, Powell TP (1970) An anatomical study of converging sensory pathways within the cerebral cortex of the monkey. *Brain* 93:793–820
- Joshua DE, Bishop PO (1970) Binocular single vision and depth discrimination. Receptive-field disparities for central and peripheral vision and the binocular interaction on peripheral single units in cat striate cortex. *Exp Brain Res* 10:389–416
- Kaas JH, Hackett TA (1998) Subdivisions of auditory cortex and levels of processing in primates. *Audiol Neurootol* 3:73–85
- Kaas JH, Hackett TA (2000) Subdivisions of auditory cortex and processing streams in primates. *Proc Natl Acad Sci USA* 97:11793–11799
- Kaas JH, Morel A (1993) Connections of visual areas of the upper temporal lobe of owl monkeys: the MT crescent and dorsal and ventral subdivisions of FST. *J Neurosci* 13:534–546
- Krubitzer LA, Kaas JH (1990) The organization and connections of somatosensory cortex in marmosets. *J Neurosci* 10:952–974
- Krumbholz K, Schonwiesner M, Von Cramon DY, Rubsamen R, Shah NJ, Zilles K, Fink GR (2005) Representation of interaural temporal information from left and right auditory space in the human planum temporale and inferior parietal lobe. *Cereb Cortex* 15:317–324
- Lee CC, Winer JA (2008) Connections of cat auditory cortex: III. Corticocortical system. *J Comp Neurol* 507:1920–1943

- Lewis JW, Van Essen DC (2000) Corticocortical connections of visual, sensorimotor, and multimodal processing areas in the parietal lobe of the macaque monkey. *J Comp Neurol* 428:112–137
- Lomber SG, MacNeil MA, Payne BR (1995) Amplification of the thalamic projections to middle suprasylvian cortex following ablation of immature primary visual cortex in the cat. *Cereb Cortex* 5:166–191
- Malhotra S, Lomber SG (2007) Sound localization during homotopic and heterotopic bilateral cooling deactivation of primary and non-primary auditory cortical areas in the cat. *J Neurophysiol* 97:26–43
- Malhotra S, Hall AJ, Lomber SG (2004) Cortical control of sound localization in the cat: unilateral cooling deactivation of 19 cerebral areas. *J Neurophysiol* 92:1625–1643
- Malhotra S, Stecker GC, Middlebrooks JC, Lomber SG (2008) Sound localization deficits during reversible deactivation of primary auditory cortex and/or the dorsal zone. *J Neurophysiol* 99:1628–1642
- Mazzoni P, Bracewell RM, Barash S, Andersen RA (1996) Spatially tuned auditory responses in area LIP of macaques performing delayed memory saccades to acoustic targets. *J Neurophysiol* 75:1233–1241
- Meredith MA, Clemo GR (1989) Auditory cortical projection from the anterior ectosylvian sulcus (field AES) to the superior colliculus in the cat: an anatomical and electrophysiological study. *J Comp Neurol* 289:687–707
- Mesulam MM (1982) Tracing neural connections with horseradish peroxidase. Wiley, Chichester
- Nikara T, Bishop PO, Pettigrew JD (1968) Analysis of retinal correspondence by studying receptive fields of binocular single units in cat striate cortex. *Exp Brain Res* 6:353–372
- Noesselt T, Rieger JW, Schoenfeld MA, Kanowski M, Hinrichs H, Heinze HJ, Driver J (2007) Audiovisual temporal correspondence modulates human multisensory superior temporal sulcus plus primary sensory cortices. *J Neurosci* 27:11431–11441
- Noppeney U (2007) The effects of visual deprivation on functional and structural organization of the human brain. *Neurosci Biobehav Rev* 31:1169–1180
- Olfert ED, Cross, BM, McWilliam AA (1993) Guide to the Care and Use of Experimental Animals. Canadian Council on Animal Care
- Olucha F, Martinez-Garcia F, Lopez-Garcia C (1985) A new stabilizing agent for the tetramethyl benzidine (TMB) reaction product in the histochemical detection of horseradish peroxidase. *J Neurosci Methods* 13:131–138
- Palmer SM, Rosa MGP (2006) A distinct anatomical network of cortical areas for analysis of motion in far peripheral vision. *Eur J Neurosci* 24:2389–2405
- Palmer LA, Rosenquist AC, Tusa RJ (1978) The retinotopic organization of lateral suprasylvian visual areas in the cat. *J Comp Neurol* 177:237–356
- Payne BR (1990) Representation of the ipsilateral visual field in the transition zone between areas 17 and 18 of the cat's cerebral cortex. *Vis Neurosci* 4:445–474
- Payne BR, Lomber SG (1996) Age dependent modification of cytochrome oxidase activity in the cat dorsal lateral geniculate nucleus following removal of primary visual cortex. *Vis Neurosci* 13:805–816
- Payne BR, Berman N, Murphy EH (1981) A quantitative assessment of eye alignment in cats after corpus callosum transaction. *Exp Brain Res* 43:371–376
- Pettigrew JD, Cooper ML, Blasdel GG (1979) Improved use of tapetal reflection for eye-position monitoring. *Invest Ophthalmol Vis Sci* 18:490–495
- Ptito M, Kupers R (2005) Cross-modal plasticity in early blindness. *J Integr Neurosci* 4:479–488
- Ptito M, Schneider FCG, Paulson OB, Kupers R (2008) Alterations of the visual pathways in congenital blindness. *Exp Brain Res* 187:41–49
- Raczkowski D, Rosenquist AC (1981) Retinotopic organization in the cat lateral posterior-pulvinar complex. *Brain Res* 221:185–191
- Rauschecker JP (1998a) Parallel processing in the auditory cortex of primates. *Audiol Neurootol* 3:86–103
- Rauschecker JP (1998b) Cortical processing of complex sounds. *Curr Opin Neurobiol* 8:516–521
- Raz N, Amedi A, Zohary E (2005) V1 activation in congenitally blind humans is associated with episodic retrieval. *Cereb Cortex* 15:1459–1468
- Reale RA, Imig TJ (1980) Tonotopic organization in auditory cortex of the cat. *J Comp Neurol* 192:265–291
- Recanzone GH (2000) Spatial processing in the auditory cortex of the macaque monkey. *Proc Natl Acad Sci USA* 97:11829–11835
- Reinoso-Suárez F (1961) Topographischer Hirnatlas der Katze für experimentell-physiologische Untersuchungen [Topographical atlas of the cat brain for experimental-physiological research]. Darmstadt: Merck.
- Rizzolatti G, Scandolara C, Matelli M, Gentilucci M (1981) Afferent properties of periarculate neurons in macaque monkeys. I. Somatosensory responses. *Behav Brain Res* 2:125–146
- Rockland KS, Ojima H (2003) Multisensory convergence in calcarine visual areas in macaque monkey. *J Psychophys* 50:19–26
- Rockland KS, Pandya DN (1979) Laminar origins and terminations of cortical connections of the occipital lobe in the rhesus monkey. *Brain Res* 179:3–20
- Roder B, Stock O, Bien S, Neville H, Rosler F (2002) Speech processing activates visual cortex in congenitally blind humans. *Eur J Neurosci* 16:930–936
- Rose JE (1949) The cellular structure of the auditory region of the cat. *J Comp Neurol* 91:409–440
- Sanderson KJ (1971) The projection of the visual field to the lateral geniculate and medial interlaminar nuclei in the cat. *J Comp Neurol* 143:101–118
- Schall JD, Morel A, King DJ, Bullier J (1995) Topography of visual cortex connections with frontal eye field in macaque: convergence and segregation of processing streams. *Vis Neurosci* 15:4464–4487
- Schlack A, Sterbing-D'Angelo SJ, Hartung K, Hoffmann K-P, Bremner J (2005) Multisensory space representations in the macaque ventral intraparietal area. *J Neurosci* 25:4616–4625
- Schroeder CE, Foxe JJ (2002) The timing and laminar profile of converging inputs to multisensory areas of the macaque neocortex. *Brain Res Cogn Brain Res* 14:187–198
- Schroeder CE, Foxe J (2005) Multisensory contributions to low-level, 'unisensory' processing. *Curr Opin Neurobiol* 15:454–458
- Schroeder CE, Lindsley RW, Specht C, Marcovici A, Smiley JF, Javitt DC (2001) Somatosensory input to auditory association cortex in the macaque monkey. *J Neurophysiol* 85:1322–1327
- Schroeder CE, Smiley J, Kaiming GF, McGinnis T, O'Connell MN, Hackett TA (2003) Anatomical mechanisms and functional implications of multisensory convergence in early cortical processing. *Int J Psychophysiol* 50:5–17
- Shipp S, Zeki S (1989) The organization of connections between areas V5 and V1 in macaque monkey visual cortex. *Eur J Neurosci* 1:309–332
- Shupert C, Cornwell P, Payne B (1993) Differential sparing of depth perception, orienting, and optokinetic nystagmus after neonatal versus adult lesions of cortical areas 17, 18, and 19 in the cat. *Behav Neurosci* 107:633–850
- Stecker GC, Mickey BJ, Macpherson EA, Middlebrooks JC (2003) Spatial sensitivity in field PAF of cat auditory cortex. *J Neurophysiol* 89:2889–2903
- Symonds LL, Rosenquist AC (1984a) Coricortical connections among visual areas in the cat. *J Comp Neurol* 229:1–38
- Symonds LL, Rosenquist AC (1984b) Laminar origins of visual corticocortical connections in the cat. *J Comp Neurol* 229:39–47

- Symonds LL, Rosenquist AC, Edwards SB, Palmer LA (1981) Projections of the pulvinar-lateral posterior complex to visual cortical areas in the cat. *Neuroscience* 6:1995–2020
- Tian B, Reser D, Durham A, Kustov A, Rauschecker JP (2001) Functional specialization in rhesus monkey auditory cortex. *Science* 292:290–293
- Tretter F, Cynader M, Singer W (1975) Cat parastriate cortex: a primary or secondary visual area. *J Neurophysiol* 38:1099–1113
- Tusa RJ, Palmer LA (1980) Retinotopic organization of areas 20 and 21 in the cat. *J Comp Neurol* 193:147–164
- Tusa RJ, Palmer LA, Rosenquist AC (1978) The retinotopic organization of area 17 (Striate Cortex) in the cat. *J Comp Neurol* 177:213–236
- Tusa RJ, Rosenquist AC, Palmer LA (1979) Retinotopic organization of areas 18 and 19 in the cat. *J Comp Neurol* 185:657–678
- Updyke BV (1983) A reevaluation of the functional organization and cytoarchitecture of the feline lateral posterior complex, with observations on adjoining cell groups. *J Comp Neurol* 219:143–181
- Updyke BV (1986) Retinotopic organization within the cat's posterior suprasylvian sulcus and gyrus. *J Comp Neurol* 246:265–280
- Watkins S, Shams L, Josephs O, Rees G (2007) Activity in the human V1 follows multisensory perception. *NeuroImage* 37:572–578
- Weeks R, Horwitz B, Aziz-Sultan A, Tian B, Wessinger CM, Cohen LG (2004) A positron emission tomographic study of auditory localization in the congenitally blind. *J Neurosci* 20:2664–2672